Measurement-Based Approach for Inertia-Trend Analysis of the US Western Interconnection

Saurav Dulal[1], Chengwen Zhang[1], Mark Baldwin[2], Qian Liu[1], Mohammed M. Olama[3], Nils M. Stenvig[3], Narayan Bhusal[3], Ajay Yadav[3], and Yilu Liu[1,3]

[1] Department of Electrical Engineering and Computer Science, The University of Tennessee, Knoxville, TN, USA
[2] Dominion Energy, Richmond, VA, USA
[3] Oak Ridge National Laboratory, Oak Ridge, TN, USA

(emails: sdulal@vols.utk.edu, and liu@utk.edu)

Abstract — **Rising deployment of inverter-based resources (IBRs), characterized by a lack of rotating mass, is decreasing the total inertia of the system. This can lead to an increased Rate of Change of Frequency (RoCoF) during the disturbance and false activation of protective devices. There is a need to assess the inertia over the past decade amidst the evolving landscape of renewable energy sources to develop strategies for integrating energy storage, enhancing resilience measures, and ensuring the stable and reliable operation of the grid. Therefore, a realistic assessment of the inertia trend using a measurement-based approach that addresses the limitations of existing models is proposed. An inertia study of the Western Interconnection in the United States is performed utilizing the data from 2013 to 2022, obtained from FNET/ GridEye network. The three-second RoCoF time window is chosen for the study as it showed an optimum balance between a strong correlation with the power imbalance (ΔP) and minimum inclusion of primary response from governor. The obtained inertia trend result shows a small percentage declination of inertia over the decade. By examining the result alongside a generation mix graph, insights are gained into the dynamic interplay between shifting energy landscape and system inertia.**

Keywords— Inertia, Inverter-Based Resources, Rate of Change of Frequency, Western Interconnection

I. INTRODUCTION

The decreasing inertia in power systems because of the increasing integration of inverter-based resources (IBRs) offers a substantial challenge to system stability. Traditionally, the usual dependence on the spinning mass of synchronous generators for inertia has proved its usefulness in reducing the Rate of Change of Frequency (RoCoF) during disturbances, hence avoiding erroneous activation of preventive mechanisms. In the context of inertial response, the power imbalance is either stored in or released from the rotating mass as kinetic energy [1]–[3]. This dynamic process is critical in rapidly stabilizing and containing the RoCoF, adding to the robustness of power system resilience and stability. However, the advent of IBRs, which are frequently characterized by grid-following behavior [4] and a lack of natural frequency response capabilities, is changing this dynamic. As these resources become more widespread, the total system inertia reduces, resulting in an increased RoCoF following disturbances. This increased RoCoF can result in the unintentional triggering of protective devices, such as under/over-frequency relays, possibly causing widespread blackouts and cascading failures [5]. Notable incidents, such as those in the United Kingdom in 2019 [6] and Australia in 2016 [7], highlight the crucial need of solving the issues posed by lower system inertia to ensure power grid stability and resilience in the face of altering energy landscapes.

As we advance toward a more sustainable future characterized by an increasing mix of renewable and clean energy sources, the energy landscape is changing significantly. The Western Interconnection in the United States, or the Western Electricity Coordinating Council (WECC), is one of the primary arenas witnessing this transformation. The history of the power mix within the WECC during the last decade demonstrates a perceptible growth in solar and wind generation, accompanied by a slight increase in gas plant output and a corresponding decline in coal plant generation [8], [9]. This transition towards a more diverse generating mix, primarily the increase in IBRs, raises critical questions concerning the trend in system inertia during this period and its consequences for grid stability. It is important to note that a thorough measurement-based method for assessing the inertia of the entire western interconnection has not yet been performed, even though analyzing the RoCoF and inertia using field-measured data offers a direct and realistic assessment of the actual and composite inertia within a system. In the past, studies [10]–[12] of the effects of variable solar and wind energy deployment have frequently relied on models to investigate how these changes affect the frequency and inertial response of the system.

Regardless of various modeling methodologies, there is a known problem in adequately portraying the complex dynamics of the complete power system. The complexity caused by the diversified generating mix, which includes IBRs, calls into question the efficacy of existing models in producing realistic outcomes. As a result, using such models alone may fall short of reflecting the subtle relationships and behaviors observed in real-world situations. The lack of a rigorous measurement-

This material is based upon work supported by the US Department of Energy, Office of Electricity (OE) under contract DE-AC05-00OR22725.

based strategy for interconnection-wide inertia analysis highlights the importance of implementing methodologies that use actual field data. Incorporating real-event data into inertia evaluations not only improves accuracy but also provides a more stable platform for understanding and managing the growing issues connected with the integration of renewable energy sources in power systems.

A measurement-based technique shown in Fig. 1 is used in this paper to undertake a comprehensive inertia trend evaluation for the WECC. The study makes use of Phasor Measurement Unit (PMU) data received from the FNET/GridEye network [13], [14] for the inertia estimation. This approach provides a solid foundation for examining the historical inertia trend during the last decade, from 2013 to 2022, by directly employing field-measured data. The results of this detailed investigation provide a quantifiable view of how inertia has evolved within the WECC throughout the chosen timeframe. The use of PMU data provides a true picture of system dynamics, allowing for a more in-depth examination of inertia changes. The study also includes a generation mix graph, which sheds light on probable reasons driving the measured inertia trends.

The remaining part of the paper is organized as follows: In Section II, the data collection source used in this study is introduced, and the preprocessing of the data before analyzing it is discussed; Section III explains the evaluation of RoCoF from the frequency data obtained after the preprocessing and the correlation between power imbalance and RoCoF for various time windows; Finally, inertia calculation and trend analysis is presented in section IV, and the paper concludes in Section V, summarizing key findings and insights.

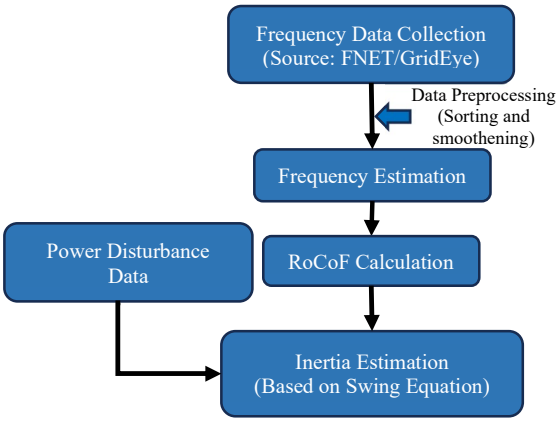

Fig. 1. Large-disturbance measurement-based inertia estimation technique.

II. Data Collection and Preprocessing

A. Data Source- FNET/GridEye

The FNET/GridEye network shown in Fig. 2 provides precise and real-time power frequency, phase angle, and voltage data collection across the USA and Canada. It is driven by more than 250 innovative Frequency Disturbance Recorders (FDRs) developed at Virginia Tech [13]. This synchronized network provides the groundwork for a thorough examination of the western interconnection, with its data server located at the University of Tennessee, Knoxville (UTK) and Oak Ridge National Laboratory (ORNL) [14].

For the particular focus on western interconnection, the study leveraged a total of 311 event trips extracted from the historical database spanning years 2013 to 2022. These rigorously gathered datasets provide unique insights into the inertia trends within the western interconnection, helping to a better knowledge of the power system dynamics and features in this region.

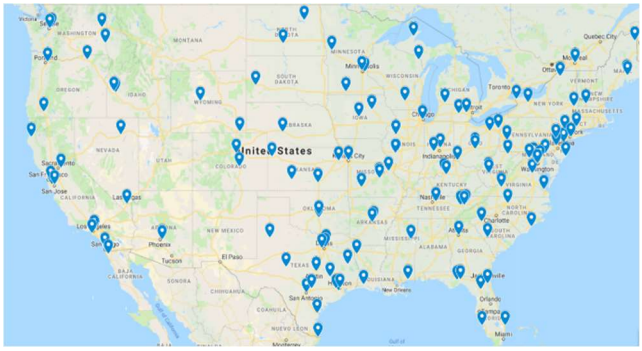

Fig. 2. Wide deployment of FNET/GridEye network in the USA.

B. Data Preprocessing

Large interconnections, such as the Western Interconnection, require a large number of measurements throughout the interconnection for reflecting the complete frequency dynamics due to its vast geographical area. Localized measurements inside constrained areas, on the other hand, may not sufficiently capture the complicated frequency dynamics that indicate the greater interconnectedness [15]. Such limited observations may give regionalized insights and oscillations unique to a certain area, but they lack the holistic perspective required to fully portray the intricacies of the entire interconnection. The median is chosen as the statistical parameter for the representation of overall system's frequency value because it is less affected by the outliers and extreme values, which are common in non-uniform sensor distributions. Unlike the mean, which can be skewed by extreme values, the median is a more representative measure of central tendency, making it appropriate for measuring interconnection frequency despite nonuniform sensor positioning.

For example, Fig. 3 illustrates the recorded frequency data curves from sensors located throughout the Western Interconnection (such as WA, ID, OR, CA, CO, UT, AZ) during an event. Notably, the blue curve denotes regional frequency dynamics particular to a region (WY), as opposed to the overall interconnection frequency. During a generation trip, marked by a red dashed line, the regional frequency drops rapidly. In contrast, the frequencies in other places decrease more gradually, which is effectively represented by the median frequency illustrated by the black curve. Therefore, determining the median frequency derived from the measurements across all the sensors proves to be crucial in representing the comprehensive frequency dynamics of the whole interconnection and mitigating oscillations.

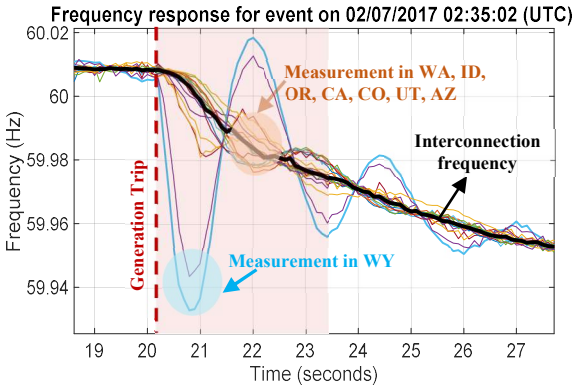

Fig. 3. Generation Trip Event plot illustrating regional and interconnection frequency.

Using (1) for each timestamp in the case of 'n' sensors, the median frequency may be simply determined, where 'F' stands for the sorted frequency list. When plotted, the resulting median frequency dataset yields a consolidated frequency plot that successfully depicts the comprehensive frequency dynamics throughout the interconnection. The representation of overall frequency behavior is made simpler by using this method.

$$f_{median} = \begin{cases} F\left[\frac{n+1}{2}\right] & \text{if n is odd} \\ \frac{F\left[\frac{n}{2}\right] + F\left[\frac{n}{2}+1\right]}{2} & \text{if n is even} \end{cases} \quad (1)$$

III. Factors Influencing RoCoF and Inertia Calculation for a Large Interconnection

The dynamics of the system shortly after a disturbance can be characterized by (2), which can be used to calculate the total inertia of the interconnection, including spinning masses, renewable energy sources, and storage devices. This formula captures the behaviors and interactions of the various parts of the system and offers a thorough framework for evaluating the properties of inertia following disruptions.

$$2H\frac{df_{median}}{dt} = (\Delta P - D\Delta f_{median}) \quad (2)$$

Here, 'H' represents the inertia constant of the entire interconnection, 'f_{median}' is the median frequency of the interconnection, 'ΔP' denotes the disturbance in power, and 'D' is the damping coefficient of the system. As the frequency change is small within the initial seconds after a generator trip, the damping component can be neglected, leading to the simplified equation:

$$\frac{df_{median}}{dt} \approx \frac{\Delta P}{2H} \quad (3)$$

A linear relationship between ΔP and the $\frac{df_{median}}{dt}$ is established by this simplified equation [15]. The inertia of the interconnection can be computed by examining the observed field data and figuring out the linear coefficient between RoCoF and ΔP. With this method, inertia may be efficiently and practically estimated from observable frequency dynamics. However, to ensure the accuracy of inertia estimation, it is crucial to have a precise evaluation of RoCoF, especially in the context of large interconnections like the WECC.

A. Evaluation of ROCOF for Large Interconnection

The huge distances across which inertial response is electromechanically transmitted create a time lag in the western interconnection's expansive power network. This lag occurs when the inertial support travels across large geographic distances to get to the disturbance's source. As a result, the dynamics of the median frequency first decline gradually and slowly, emphasizing the delayed arrival of inertial support from far-off regions to the source of disturbance. The blue curve that shows a sharp decline in Fig. 3 is the regional frequency at the event location. As a result, the dynamics of the regional frequency can be efficiently captured by computing the RoCoF within a brief time frame. The median frequency, on the other hand, remains fairly constant until the blue curve reaches its nadir. As inertia support from diverse locations of the interconnection is received after this point, the median frequency progressively begins to decline.

Given the delayed reaction in the median frequency, a larger time window may be required to correctly reflect the interconnection frequency dynamics. The network's significant overall inertia contributes to a lower RoCoF during the early stages of a disturbance. However, the smaller RoCoF increases sensitivity to noise, especially when using a short time window. Balancing the trade-off between time window size and sensitivity becomes critical for a thorough and accurate examination of the frequency dynamics of the interconnection. A careful balance must be found when selecting the right time window to capture the inertial response in the vast interconnection, since too-long time windows may inadvertently include the primary response from governor.

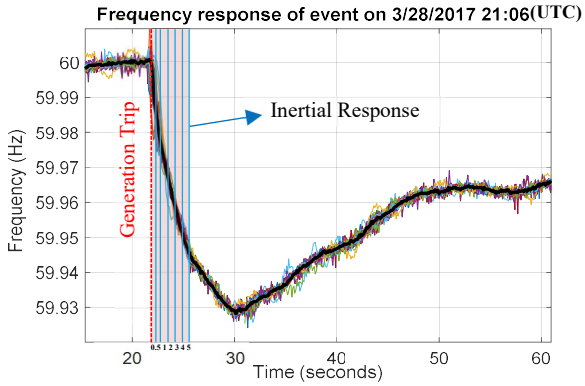

Fig. 4. Frequency response of a sample event illustrating RoCoF calculation at various time windows capturing inertial response.

A practical method is to utilize the correlation coefficient as an indicator to guide the selection of an optimal time window. Once the median frequency is determined, the start time of an event shown by red dashed line in Fig. 4 is detected automatically by a program. RoCoF readings are calculated at several time periods ranging from 0.5 to 5 seconds using (4). The blue lines in Fig. 4 indicate several time windows for RoCoF calculation. The correlation coefficient between RoCoF and power imbalance (MW) obtained from NERC confirmed

event list is calculated for each time window. This gives a quantitative measure of the link between RoCoF and power imbalance, assisting in the selection of the most appropriate time window that efficiently captures the inertial response while reducing the effects of primary governor reactions.

$$\mathrm{RoCoF}_{T_{\mathrm{interval}}} = \frac{f_{t_{\mathrm{start}}} - f_{t_{\mathrm{start}}+T_{\mathrm{interval}}}}{T_{\mathrm{interval}}} \quad (4)$$

where $f_{t_{start}}$ is the frequency just before start of the event, $T_{interval}$ represents different time windows: 0.5, 1, 2, 3, 4 and 5 sec after the start of the event.

B. Correlation Coefficient and Time Window Selection

The correlation coefficient (R) measures the consistency in the linear relationship between megawatt (MW) size and RoCoF and acts as a reliability measure for RoCoF time window estimate. A high R-value implies a strong linear relationship, that can effectively filter out the primary frequency response from the governor determining the best time window for accurate estimation. This metric also ensures that the selected time window captures significant dynamics without introducing irrelevant noise. The RoCoF, which is calculated for each occurrence over a set time window, can be correlated with MW sizes as (5).

$$R = \frac{1}{N-1}\sum_{i=1}^{N}\left(\frac{MW(i)-\mu_{MW}}{\sigma_{MW}}\right)\left(\frac{RoCoF(i)-\mu_{RoCoF}}{\sigma_{RoCoF}}\right) \quad (5)$$

where *R* is the correlation coefficient, *N* is the number of events, *MW* is the vector of MW sizes for generation trip events, *RoCoF* is the vector of RoCoFs calculated for specified time window, μ_{MW} and μ_{RoCoF} are the average values of the *MW* and *RoCoF* vectors, and σ_{MW} and σ_{RoCoF} are the standard deviations of the *MW* and *RoCoF* vectors.

Fig. 5. shows a distinct pattern in which the correlation coefficient increases with increasing RoCoF time windows ranging from 0.5 sec to 5 sec. At the same time, the average correlation coefficient is increasing, while the standard deviation is decreasing. A 3-second time limit emerges as an appropriate option for maintaining a balance and avoiding capturing the primary response. This period provides a desirable equilibrium, ensuring a strong correlation while minimizing the governor's active participation in the system's reaction dynamics.

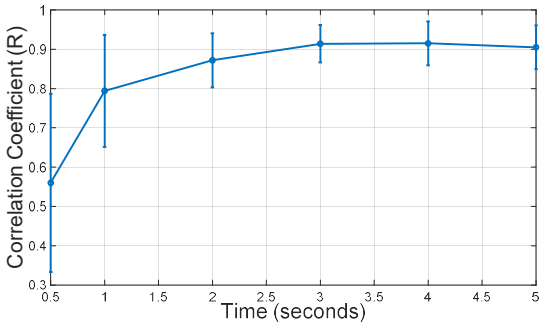

Fig. 5. Mean values of correlation coefficient with standard deviation error bars for different time windows.

C. Outliers

When data from a sample year is analyzed, it becomes clear that certain outlier events depart significantly from the established patterns seen in the majority of cases. To provide an accurate assessment of system inertia, it is critical to adopt a thorough approach for finding, analyzing, and justifying the exclusion of these outliers. Outliers are often classified into two types: those caused by soft trip occurrences and those discovered using statistical screening procedures with no apparent cause.

Soft trip events, which particularly pose difficulty in accurate inertia computation, are distinguished by a staged disconnection process. This begins with the shutdown of the prime mover, which could be any type of turbine (gas, steam, or hydro). Following this, there is a gradual ramp-down of MW output before the generator disconnects. This disconnection process, in which power production slowly drops after the quick shutdown of the turbine, frequently results in data points migrating to the left side of the MW-ROCOF plane. Such adjustments can dramatically alter inertia estimations. Fig. 6(a) depicts a typical normal trip event with a distinct frequency turning point followed by a quick, clear frequency drop. A soft trip event as illustrated in Fig. 6(b), on the other hand, has a more rounded frequency turning point with a gradual decrease. This subtle distinction highlights the issue that soft trip events can impact the precision of inertia computations. Outliers in the second category can be effectively identified and excluded using some statistical techniques or visual inspection. This is frequently accomplished by looking for anomalies in the MW vs. RoCoF plot that are far from the fitted line.

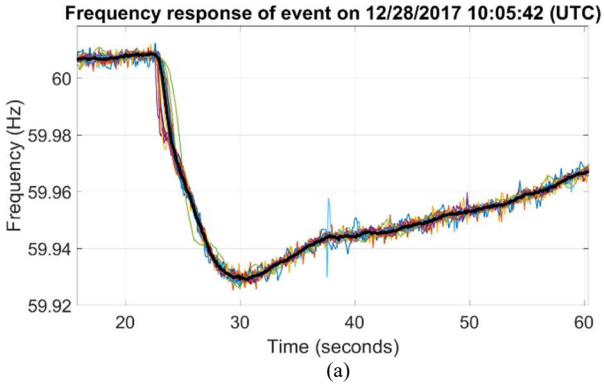

(a)

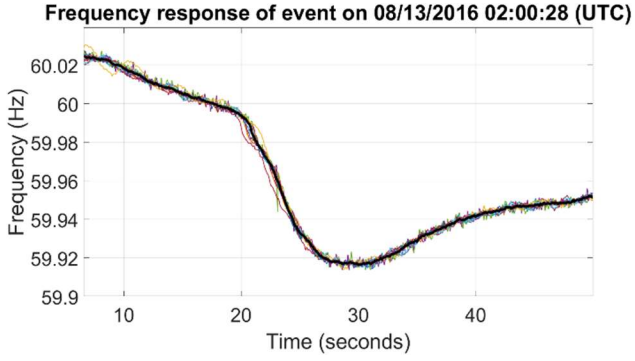

(b)

Fig. 6. (a) Normal trip event (b) Soft trip event.

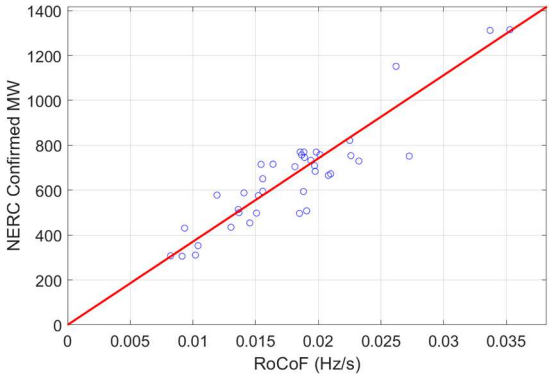

Fig. 7. Scatter plot of MW vs. RoCoF for 2016.

The entire method entails a meticulous manual examination of each event's frequency plot, with only those events having a clear turning point being chosen. This stage is critical for enhancing the dataset and improving the correlation between MW and RoCoF, resulting in a more precise measurement of inertia. By removing anomalous events that deviate from regular patterns, the dataset becomes more indicative of the actual dynamics of the power system, ensuring that calculated inertia values closely resemble actual conditions. Fig. 7 illustrates a scatter plot of MW versus RoCoF with a fitted line, excluding all identified outliers for the year 2016. The noteworthy improvement in the correlation coefficient, rising from 0.75 to 0.9, underscores the effectiveness of omitting these outliers as tabulated in Table I. Consequently, the events remaining in the plot can be considered robust and conducive to accurately estimating inertia, as they contribute to a stronger and more reliable correlation between MW and RoCoF.

TABLE I. CORRELATION COEFFICIENT WITH AND WITHOUT OUTLIERS FOR 2016

Events	Correlation Coefficient (R)	Remarks
With Outliers	0.75	Moderate
Without Outliers	0.9	Strong

IV. INERTIA EVALUATION & TRENDS

A. Inertia Calculation

Once the parameters for power imbalance and RoCoF are known, inertia can be easily determined using (3). The inertia value can be calculated directly from the slope of the red fitted line in the MW versus RoCoF plot using the best 3-second time window as discussed earlier. To find out the quarterly inertia values of a year, the events occurring in each quarter are utilized to implement the least square fitting method to find first-order fitted curves which slopes represent their respective quarterly inertia. The following expression implements the method:

$$2\hat{H} = (\mathrm{RoCoF}^{\mathrm{T}}\mathrm{RoCoF})^{-1} \cdot \mathrm{RoCoF}^{\mathrm{T}} \cdot \mathrm{MW}$$
$$\text{where} \quad \mathrm{RoCoF} = \left[\frac{\Delta f_1}{\Delta t}, \frac{\Delta f_2}{\Delta t}, \ldots, \frac{\Delta f_n}{\Delta t}\right]^{\mathrm{T}} \qquad (6)$$
$$\mathrm{MW} = [\mathrm{MW}_1, \mathrm{MW}_2, \ldots \mathrm{MW}_n]^{\mathrm{T}}$$

In (6), *RoCoF* represents the vector of the rate of change of frequency $(\Delta f_i/\Delta t)$ for each generation trip event i over a specified time window Δt. The vector *MW* corresponds to the sizes of the respective generation trip events, denoted as MW_i.

B. Inertia Trends & Analysis

The inertia calculation was carried out for each year from 2013 to 2022, utilizing field data collected throughout several parts of the Western Interconnection. Fig. 8 depicts the inertia trend over the last decade, with each blue circle representing quarterly inertia values of each year. The inertia trend from 2013 to 2022 is drawn out by connecting these blue circles with blue lines. The red line is a smoothed trendline that depicts the overall decrease in inertia across the whole period.

A closer analysis of the graph reveals that the inertia of the Western Interconnection remained essentially steady across the decade, with an approximately 10% decline observed. In addition, the graph shows that inertia levels are mostly higher during the third quarter of the year. This trend can be associated with the increased number of generators connected to the system during the summer months, highlighting the seasonal variation in inertia levels within the Western Interconnection.

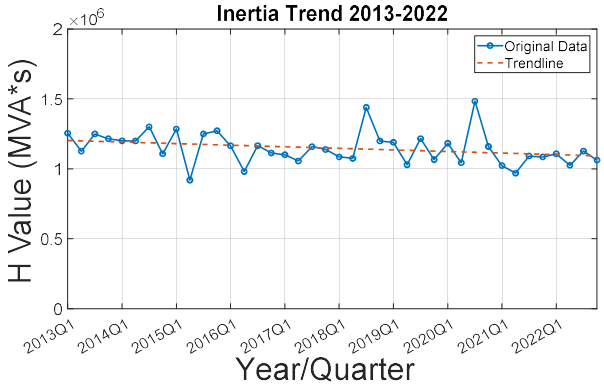

Fig. 8. Inertia trend of the Western Interconnection 2013-2022.

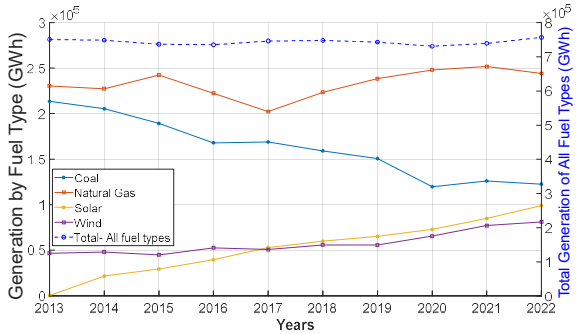

Fig. 9. Generation portfolio graph of the Western Interconnection 2013-2022.

Despite greater integration of renewable energy sources, there is a small percentage decline in inertia. This is intriguing and can be traced in part to changes in the generation mix profile. This is evident in Fig. 9, where the data, sourced from [8], illustrates the changes in unit commitment patterns. There has been a slight increase in generation from gas units that could contribute to the part in offsetting the inertia decrease. Although there has been a decrease in coal unit generation over

the last decade, many coal plants may continue to operate at lower outputs, retaining a relatively same number of online rotating mass. Furthermore, some renewable resources can respond quickly to frequency changes, thanks to inverter controls. While the quantity of rapid frequency support available from renewables today remains minimal, their impact on real frequency is unknown.

Understanding these complexities within the context of changing generation profiles is critical for operators and planners. In the face of shifting energy landscapes, strategies such as energy storage integration, better controls, and resilience measures become critical for sustaining grid stability and assuring dependable system operation. This demands understanding the system's current state, which is effectively met by the measurement-based approach of study discussed herein.

V. Conclusion

In this paper, the inertia trend analysis over the last decade is carried out utilizing historical field measurement data from the entire Western Interconnection. The median frequency data is used to precisely depict the frequency dynamics of the system, reducing the influence of regional frequency oscillations. Various time windows are carefully investigated for predicting RoCoF, and a 3-second time window emerged as optimum, displaying a good association with MW values. While the 3-second time window is acknowledged to have the potential for primary response effects, the impact on the results is mitigated by the explicit focus on inertia trend analysis and the percentage decrease over time. Rather than targeting instantaneous responses, the emphasis in this instance is on capturing broader patterns of inertia behavior and assessing the overall trajectory over the decade. This method enables a more robust and relevant assessment of the system's inertia dynamics of the WECC while considering changes in the energy-generating landscape.

Acknowledgment

This manuscript has been authored by UT-Battelle, LLC, under contract DE-AC05-00OR22725 with the US Department of Energy (DOE). The US government retains and the publisher, by accepting the article for publication, acknowledges that the US government retains a nonexclusive, paid-up, irrevocable, worldwide license to publish or reproduce the published form of this manuscript, or allow others to do so, for US government purposes. DOE will provide public access to these results of federally sponsored research in accordance with the DOE Public Access Plan (https://www.energy.gov/doe-public-access-plan).

References

[1] V. Vittal, J. D. McCalley, P. M. Anderson, and A. A. Fouad, *Power system control and stability,* in IEEE Press Series on Power and Energy Systems. Wiley, 2019. [Online]. Available: https://books.google.com/books?id=obCuDwAAQBAJ

[2] P. Denholm, T. Mai, R. Kenyon, B. Kroposki, and M. O'Malley, *"Inertia and the power grid: A guide without the spin,"* Technical Report, National Renewable Energy Laboratory, NREL/TP-6A20-73856, 1659820, MainId:6231, May 2020. doi: 10.2172/1659820.

[3] P. Kundur, N. J. Balu, and M. G. Lauby, "*Power system stability and control,"* in EPRI power system engineering series. McGraw-Hill Education, 1994. [Online]. Available:https://books.google.com/books?id=wOlSAAAAMAAJ

[4] *"Grid forming inverter study Report."* WECC Technical Report, Accessed: Jan. 05, 2024. [Online]. Available: https://www.wecc.org/Administrative/Grid%20Forming%20Inverter%20Study%20Report.pdf

[5] B. Tan, J. Zhao, M. Netto, V. Krishnan, V. Terzija, and Y. Zhang, "Power system inertia estimation: Review of methods and the impacts of converter-interfaced generations," *Int. J. Electr. Power Energy Syst.*, vol. 134, p. 107362, Jan. 2022, doi: 10.1016/j.ijepes.2021.107362.

[6] *"9_august_2019_power_outage_report."* Accessed: Jan. 05, 2024. [Online]. Available: https://www.ofgem.gov.uk/sites/default/files/docs/2020/01/9_august_2019_power_outage_report.pdf

[7] *"Black system event compliance report - Investigation into the pre-event system restoration and market suspension aspects surrounding the 28 September 2016 event"* Accessed: Jan. 05, 2024. [Online]. Available: https://www.aer.gov.au/system/files/Black%20System%20Event%20Compliance%20Report%20-%20Investigation%20into%20the%20Pre-event%20System%20Restoration%20and%20Market%20Suspension%20aspects%20surrounding%20the%2028%20September%202016%20event.pdf

[8] "*Electricity data browser - Net generation for all sectors."* Accessed: Jan. 05, 2024. [Online]. Available: https://www.eia.gov/electricity/data/browser/

[9] *"Looking Beyond the Region: US and the Western Interconnect."* Accessed: Jan. 05, 2024. [Online]. Available: https://www.nwcouncil.org/2021powerplan_wecc-existing-system-and-retirements/

[10] J. Tan, Y. Zhang, S. You, Y. Liu, and Y. Liu, "Frequency Response Study of U.S. Western Interconnection under Extra-High Photovoltaic Generation Penetrations," in 2018 *IEEE Power & Energy Society General Meeting (PESGM)*, Portland, OR: IEEE, Aug. 2018, pp.15. doi:10.1109/PESGM.2018.858613.

[11] *"Changes in System Inertia (Final)."* Accessed: Jan. 05, 2024. [Online].Available:https://www.wecc.org/Reliability/Changes%20in%20System%20Inertia%20(Final).pdf

[12] Y. Liu, S. You, J. Tan, Y. Zhang, and Y. Liu, "Frequency response assessment and enhancement of the U.S. power grids toward extra-high photovoltaic generation penetrations—An industry perspective," *IEEE Trans. Power Syst.*, vol. 33, no. 3, pp. 3438–3449, May 2018, doi: 10.1109/TPWRS.2018.2799744.

[13] Y. Liu *et al.*, "Recent developments of FNET/GridEye — A situational awareness tool for smart grid," *CSEE Journal of Power and Energy Systems*, vol. 2, no. 3, pp. 19-27, Sept. 2016, doi: 10.17775/CSEEJPES.2016.00031.

[14] Y. Zhang, P. Markham, T. Xia, L. Chen, Y. Ye, Z. Wu, Z. Yuan, L. Wang, J. Bank, J. Burgett, R. W. Conners, and Y. Liu, "Wide-area frequency monitoring network (FNET) architecture and applications," *IEEE Trans. Smart Grid*, vol. 1, no. 2, pp. 159-167, July 2010.

[15] C. Zhang, "Measurement-based monitoring and control in power systems with high renewable penetrations," PhD diss., University of Tennessee, 2023.